Bioorganic & Medicinal Chemistry Letters 25 (2015) 616–620

Contents lists available at ScienceDirect

Bioorganic & Medicinal Chemistry Letters

journal homepage: www.elsevier.com/locate/bmcl

Discovery of *O*-(3-carbamimidoylphenyl)-L-serine amides as matriptase inhibitors using a fragment-linking approach

Rajeev Goswami [a], Gerd Wohlfahrt [b], Subhendu Mukherjee [a], Chakshusmathi Ghadiyaram [a], Jwala Nagaraj [a], Leena K. Satyam [a], Krishnaprasad Subbarao [a], Sreevalsam Gopinath [a], Narasimha R. Krishnamurthy [a], Hosahalli S. Subramanya [a], Murali Ramachandra [a,*]

[a] *Aurigene Discovery Technologies Limited, 39-40 KIADB Industrial Area, Electronic City Phase II, Bangalore 560 100, India*
[b] *Orion Corporation, Orionintie 1, FIN-02101 Espoo, Finland*

ARTICLE INFO

Article history:
Received 2 September 2014
Revised 2 December 2014
Accepted 4 December 2014
Available online 17 December 2014

Keywords:
Fragment-linking approach
Matriptase
Molecular docking
Crystallography
Anti-tumor

ABSTRACT

Matriptase is a cell-surface trypsin-like serine protease of epithelial origin, which cleaves and activates proteins including hepatocyte growth factor/scatter factor and proteases such as uPA, which are involved in the progression of various cancers. Here we report a fragment-linking approach, which led to the discovery of *O*-(3-carbamimidoylphenyl)-L-serine amides as potent matriptase inhibitors. The co-crystal structure of one of the potent inhibitors, **6** in complex with matriptase catalytic domain validated the working hypothesis guiding the development of this congeneric series and revealed the structural basis for matriptase inhibition. Replacement of a naphthyl group in **6** with 2,4,6-tri-isopropyl phenyl resulted in **10** with improved matriptase inhibition, which exhibited significant primary tumor growth inhibition in a mouse model of prostate cancer. Compounds such as **10**, identified using a fragment-linking approach, can be explored further to understand the role of matriptase as a drug target in cancer and inflammation.

Tumor development is the pathologic outcome of uninhibited invasive growth in which proteases play a vital role. Proteases not only mediate degradation of extra-cellular matrix and inter-cellular cohesive structures allowing migration of cells into the extra-cellular surroundings, but also stimulate various angiogenic factors and cell growth. A type II transmembrane trypsin-like serine protease, viz., matriptase, overexpressed in many human cancers is known to contribute substantially to this process.[1] Matriptase also activates proteases such as uPA that plays a critical role in angiogenesis, tumor invasion and metastasis. Down-regulation of matriptase is known to inhibit tumor invasion through uPA receptor repression.[2,3] Hence, a therapeutic strategy for preventing tumor growth and migration could be through matriptase inhibition.

Matriptase is also known to be overexpressed in inflammatory conditions such as osteoarthritis,[4] or specifically activated in several inflammatory skin disorders.[5] However matriptase is down-regulated in other inflammatory conditions including Crohn's disease and ulcerative colitis.[6] Recent findings suggest that matriptase proteolytically activates hemagglutinin of H9N2 and H1N1 influenza A viruses and promotes multicycle viral replication in the human airway epithelium.[7,8]

In the past few years, several groups have disclosed small molecule matriptase inhibitors. Among them Curacyte GmbH has published comprehensive studies covering amidinophenylalanines,[9–11] which showed moderate anti-tumor efficacy in a xenograft efficacy model. Peptidomimetic matriptase inhibitors[12,13] based on the P4–P1 section of the activation peptide of matriptase have also been reported. Bis-benzamidine analogues of hexamidine[4] that exhibited moderate matriptase binding affinity have also been reported. We recently published novel tri-substituted pyridyl[14] and benzene[15] based potent and selective matriptase inhibitors, which exhibited significant inhibition of migration and invasion with several prostate cancer cell lines. Furthermore, selected compounds also displayed significant primary tumor growth inhibition in a prostate cancer xenograft mouse model.[15]

The matriptase catalytic domain reveals a trypsin-like serine proteinase fold, featuring a unique 60-insertion loop region that influences interactions with protein substrates. The structure divulges a trypsin-like S1 cavity, a small hydrophobic S2 subpocket and a solvent exposed spacious S4 region.[16] In the present study, we sought to utilize a fragment-linking approach for

* Corresponding author. Tel.: +91 80 7102 5444; fax: +91 80 2852 6285.
E-mail address: murali_r@aurigene.com (M. Ramachandra).

http://dx.doi.org/10.1016/j.bmcl.2014.12.008
0960-894X/

identification of matriptase inhibitors. Screening of our in-house library of benzamidine analogs (MW <300) in a biochemical assay resulted in the identification of weak hits (**1** and **2**) exhibiting a matriptase K_i[17] of ≈80 μM. Fragments **1** and **2** showed potential for further development because of their low molecular weight, presence of a single amidine group and moderate matriptase binding affinity. We decided to retain one amidine functionality in further designs because several co-crystal structures indicated that an amidine group is an important binding feature for making strong salt-bridge interactions with Asp189 in the S1 pocket.[9–11,14–16] Both **1** and **2** were modeled in the matriptase catalytic domain (cd) which predicted the phenyl sulfonamide (**1**) and piperidyl ethyl amine (**2**) projecting towards S2/S4 and S1′ regions, respectively, with the amidine moiety making salt-bridge interaction with Asp189 in S1 pocket, as observed in the crystallographic binding mode of benzamidine (Fig. 1a).[16] Apart from these, the models suggested opportunities for further optimization including binding affinity improvement through incorporation of more hydrophobic groups on the pendant benzene in **1** because this moiety is expected to occupy space in the vicinity of Phe99 and Trp215 (Fig. 1a). Therefore, an analog (**3**) was synthesized replacing the terminal benzene with naphthyl. Fragment **3** exhibited 3-fold improvement in matriptase inhibition compared to **1**. We further wanted to explore if fragments **1** and **3** can be linked at the ethoxy β-carbon (∂, Fig. 1a) into a single compound having groups orienting towards three distinct regions of the matriptase cd, viz., S1, S2/S4 and S1′ sites, then this might create more (specific?) interactions and improve binding affinity. This fragment-linking approach required SAR studies to map these three separate regions since this approach has not been explored in earlier publications.

The synthesis of *O*-(3-carbamimidoylphenyl)-L-serine amides is outlined in Scheme 1. Methyl L-serinate was sulfonylated using arylsulfonyl chloride with NMM (*N*-methylmorpholine) in THF resulting in sulfonamide **13**, which was further hydrolyzed using LiOH to obtain acid **14**. Commercially available amines were coupled with acid **14** using 1-ethyl-3-(3-dimethylaminopropyl)carbodiimide (EDCI) to obtain **15**. The free hydroxyl group of **15** was mesylated with methanesulfonyl chloride to give **16**, which was coupled with 3-hydroxybenzonitrile and resulted in 3-cyanophenoxy analog **17**. Treatment of nitrile group of **17** with aq NH_2OH[14] in EtOH converted it to *N*-hydroxyamidine (**18**), followed by acetylation to form *N*-acetoxyamidine (**19**) which was further reduced to afford amidine **20**. The Boc-protected amino group (if present) was deprotected using ethanolic-HCl to give the desired compounds.

Based on the fragment linking approach, compounds **4** and **5** were synthesized (Fig. 1a). Compound **4** (*R* isomer) showed poor matriptase inhibition but **5** (*S* isomer) exhibited 11 and 3-fold improved inhibition compared to **2** and **3**, respectively, with a K_i of 7.4 μM. This modification demonstrated the importance of stereo-chemistry for binding and also validated our model-based hypothesis for linking fragments **1** and **3**. Although compound **5** exhibited better matriptase inhibition than **2** and **3**, there was room for further improving its inhibitory activity based on the missing polar contacts involving the P2/P4 and P1′ ends as shown in Figure 1a. This idea was also supported by earlier publications[9,14,15] that highlighted the importance of polar interactions in the S2–S4 and S1′ regions for binding affinity improvement.

Compound **5** was docked in the matriptase catalytic domain, which suggested a binding mode resembling to **2** and **3** (Fig. 1b) with a possibility of introducing polar contacts with S2/S4 or S1′ residues. This compound **5** model also suggested that moving the amidine group from *para* to *meta* position might shift the sulfonamide and carbonyl groups closer to the backbones of Trp215, Gly216 and Gly219 and gain additional polar interactions (Fig. 2a). This modification was nevertheless anticipated to compromise the critical catalytic Ser195 contact which the ether oxygen of **5** is expected to engage (Fig. 1a) but at the same time result in additional polar interactions with S2/S4 or S1′ potentially leading to improved binding and target inhibition. With this hypothesis, compound **6** (Table 1) was synthesized and it showed significant improvement of 25-fold in matriptase inhibition. A high resolution (1.9 Å) crystal structure of **6** in complex with matriptase showed that P1′ ethyl amine interacts with His57 through a water molecule and the P1 amidine binding in the S1 pocket result in a number of polar contacts. Most importantly, the ether oxygen does not make any contact with Ser195 (but interacts with Gln192 instead), and the sulfonamide and carbonyl interact with the backbones of Trp215, Gly216 and Gly219 residues.

The significantly improved matriptase inhibition observed with **6** and its experimentally determined binding mode with matriptase motivated us to further study the SAR for different P1′ and P4 groups, which are described in Table 1. Initially, compounds **7** and **8** with different P1′ groups were synthesized to understand the role of water-mediated interaction with His57 observed for

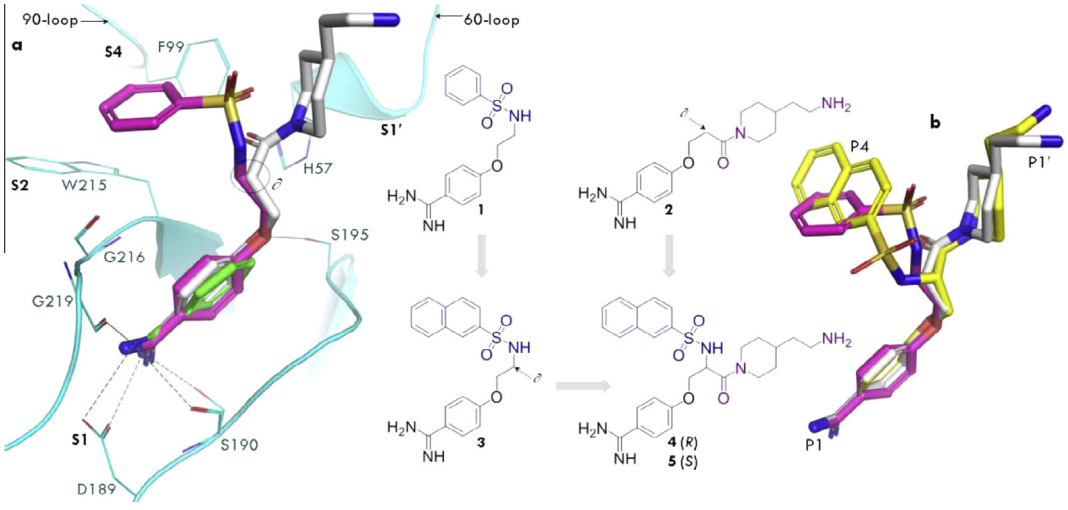

Figure 1. (a) Predicted binding modes of **1** (pink) and **2** (gray) compared to the crystallographic binding mode of benzamidine (green) in matriptase cd (PDB ID: 1EAX). Water mediated interactions involving benzamidine not shown for clarity. indicates linking region for hybrid compounds **4** and **5**; (b) overlay of the docked models of **1** (pink), **2** (gray) and **5** (yellow). Benzamidine, **1**, **2**, **3**, **4** and **5** showed K_i of 400 μM (approx.), 78.8 μM, 80.7 μM, 25.4 μM, 98.6 μM and 7.4 μM, respectively, for matriptase.

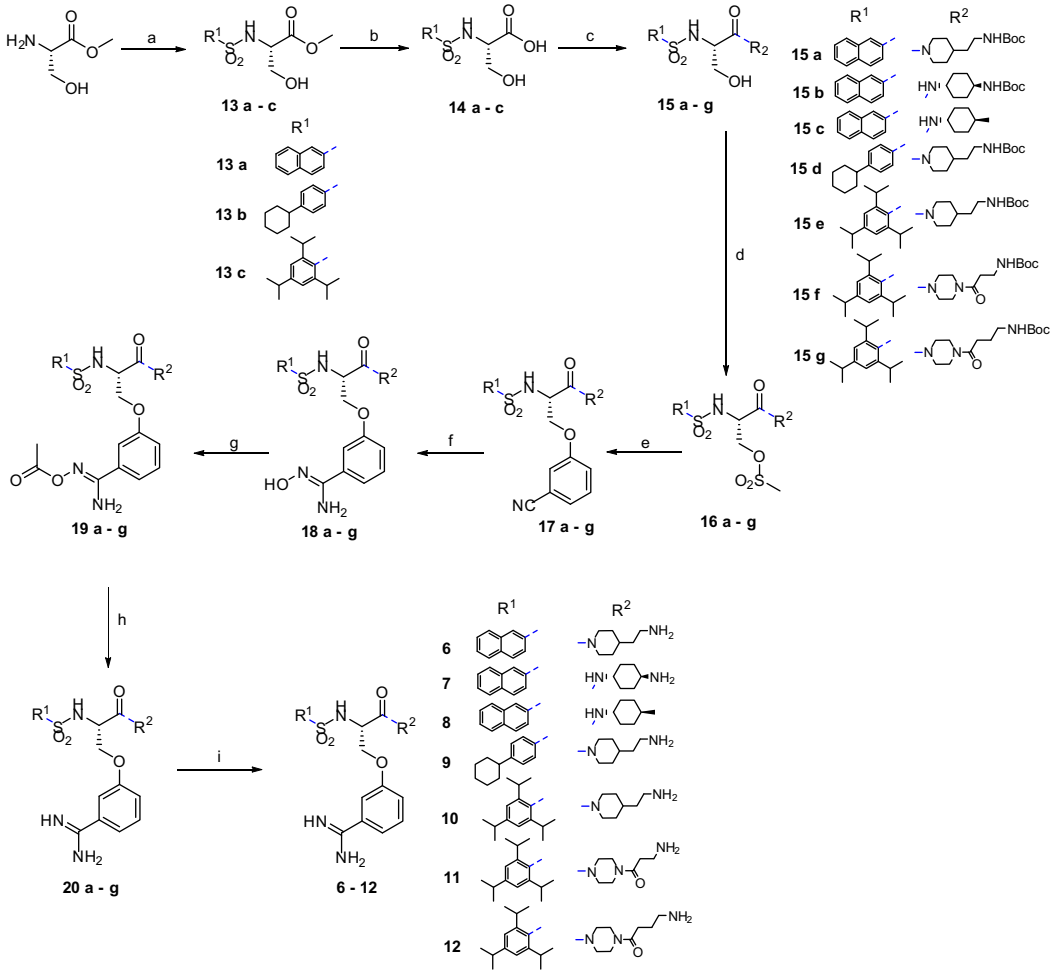

Scheme 1. Synthetic Scheme of *O*-(3-carbamimidoylphenyl)-L-serine amides. Reagents and conditions: (a) arylsulfonyl chloride, NMM, THF, 10 h, rt; (b) LiOH, THF, MeOH, 2 h, 15–20 °C; (c) cycloalkyl amine (with or without pendant amine masked with Boc), EDCI, HOBt, DIPEA, DMF, 12 h, rt; (d) methanesulfonyl chloride, TEA, DCM, 2 h, rt; (e) 3-hydroxybenzonitrile, K_2CO_3, DMF, 6 h, 70 °C; (f) aq NH_2OH, EtOH, 4 h, 75 °C; (g) Ac_2O, AcOH, 4 h, rt; (h) Zn powder, AcOH, 4 h, rt; (i) $HCl_{(gas)}$–EtOH, 2 h, 5–10 °C.

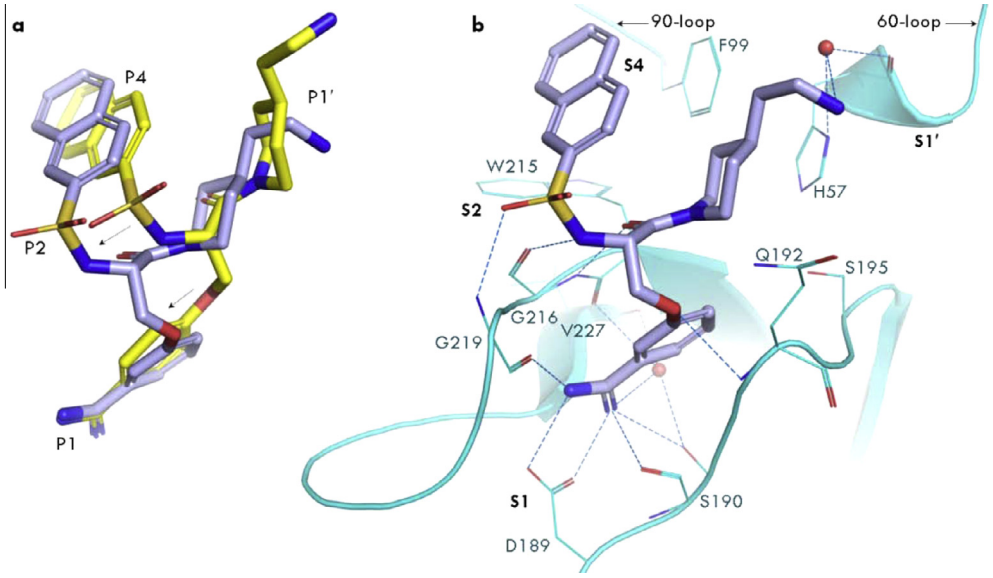

Figure 2. (a) Overlay of the docked model of **5** (yellow) and crystallographic binding mode of **6** (light blue) in matriptase cd and (b) key interactions and orientation of different groups as observed in the crystallographic binding mode of **6** (light blue) in matriptase cd (PDB ID: 4R0I). Red spheres indicate crystallographic waters.

Table 1
P4 and P1′ SAR of *O*-(3-carbamimidoylphenyl)-L-serine amides

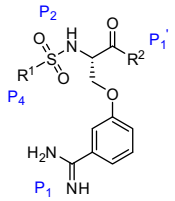

ID	R^1	R^2	K_i[a] (μM)/% *inhibition*[b] at 5 μM		
			Matriptase	uPA	Plasmin
6	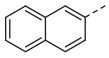	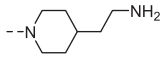	0.3	*9%*	*23%*
7	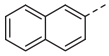	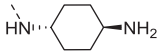	3.7	*2%*	*22%*
8	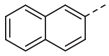	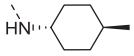	*13%*	nd[c]	nd[c]
9	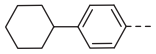	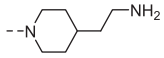	0.3	*3%*	*14%*
10	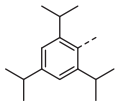	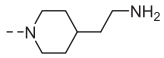	0.1	*5%*	*26%*
11	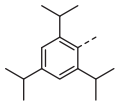	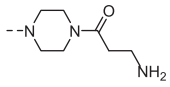	1.7	*6%*	*28%*
12	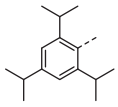	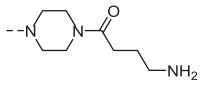	1.5	*8%*	*9%*

[a] K_i: mean of at least two independent experiments with standard deviation within ± 10%.
[b] % inhibition: K_i was not determined for compounds which show ⩽30% inhibition at 5 μM concentration.
[c] nd: not determined against the mentioned enzyme.

Table 2
Analysis of selected compounds for functional activity on DU-145 cells, aqueous solubility, metabolic stability and PK profile

ID	% cytotoxicity with DU-145 at 10 μM	Inhibition of DU-145 (% inhibition[a] at 10 μM)		aq sol[a] (μM) at pH 7.4	MLM stability[a] (% parent remaining)		Subcutaneous PK[b] at 1 mg/kg			
		Migration	Invasion		20 min	40 min	T_{max} (h)	C_{max} (ng/ml)	Beta $t_{1/2}$ (h)	AUC (0–inf) (ng h/ml)
6	8	58 ± 3.2	70 ± 6.8	180 ± 4	82 ± 2	61 ± 4			nd[c]	
9	18	32 ± 2.8	39 ± 6.0	151 ± 8	80 ± 7	52 ± 4				
10	4	85 ± 6.1	92 ± 8.2	178 ± 6	95 ± 6	85 ± 7	0.25	337	0.9	433

[a] Values represent mean ± SD.
[b] Male NMRI mice were dosed subcutaneous at 1 mg/kg with compound formulated with 100% PBS.
[c] nd: not determined.

compound **6** (Fig. 2b). Compound **7** with 4-amino cyclohexane P1′ moiety displayed a 12-fold reduced affinity while a similar compound **8** with 4-methyl cyclohexane group showed >40 fold reduced binding affinity underscoring the importance of P1′ interaction. Furthermore, the binding mode of **6** showed that the P4 naphthyl group is hydrophobically enclosed between Phe99 and Trp215 (Fig. 2b). We therefore explored other hydrophobic groups and synthesized compounds **9** and **10**. Compound **9** with 4-cyclohexylphenyl did not exhibit any improvement while compound **10** with 2,4,6-tri-isopropylphenyl group showed 3 fold improved inhibitory activity (K_i = 0.1 μM) compared to **6** and suggested that tri-isopropylphenyl is a better S4 binder than naphthyl. Therefore additional compounds with extended alkyl amine P1′ groups (R_2) retaining R_1 as tri-isopropylbenzene **11** and **12** were synthesized to evaluate whether longer alkyl amine side-chains can also engage in the same water-mediated interaction with His57 (Fig. 2b) but both compounds showed reduced potency. When these compounds were tested in an in-house serine protease panel, good selectivity against uPA and plasmin was observed (Table 1).

After establishing the SAR for matriptase inhibition and selectivity against uPA and plasmin, selected compounds were evaluated for their functional activity in matriptase expressing prostate carcinoma cell line DU-145,[18] solubility and metabolic stability in mouse liver microsomes (Table 2). Overexpression of matriptase with concomitant loss of HAI-1potentially contributing to the aggressiveness of prostate carcinoma cell lines including DU-145, an androgen-independent prostate carcinoma cells when compared to normal human prostate epithelial cells has been reported.[18]

Compounds **6** and **10** at non-cytotoxic concentrations showed good inhibition of invasion and migration of DU-145 cells. All three compounds have high aqueous solubility, but **10** exhibited better metabolic stability and therefore **10** was selected for in vivo mouse pharmacokinetic studies. Although in the subcutaneous PK study at 1 mg/kg dose, compound **10** showed only moderate exposure, in order to understand its role in anti-tumor activity it was taken up further for in vivo efficacy studies. When compound **10** was dosed subcutaneously at 1 mg/kg once daily for 28 days in SCID mice bearing subcutaneous DU-145 prostate cancer xenograft tumors, it exhibited significant inhibition of the primary tumor growth of 57%. Additionally, none of the mice treated with compound **10** showed any significant weight loss (<5%) or other clinical signs of toxicity.

In summary, we have explored a fragment-linking approach and developed novel *O*-(3-carbamimidoylphenyl)-L-serine amides and achieved good potency for matriptase both in enzymatic and cellular assays, and selectivity against uPA and plasmin. One of the selected compounds (**10**) also showed significant primary tumor growth inhibition in a DU-145 prostate cancer xenograft model. Compound **10** has further potential to be explored as a tool to understand the role of matriptase in various cancers, inflammation[4] and influenza A viruses[6,7] where matriptase is reported to play a key role.

Acknowledgment

We gratefully acknowledge Orion Corporation for funding this research.

Supplementary data

Supplementary data associated with this article can be found, in the online version, at http://dx.doi.org/10.1016/j.bmcl.2014.12.008. These data include MOL files and InChiKeys of the most important compounds described in this article.

References and notes

1. Uhland, K. *Cell. Mol. Life Sci.* **2006**, *63*, 2968.
2. Suzuki, M.; Kobayashi, H.; Kanayama, N.; Saga, Y.; Suzuki, M.; Chen-Yong, L.; Dickson, R. B.; Terao, T. *J. Biol. Chem.* **2004**, *279*, 14899.
3. Sheau-Ling, L.; Dickson, R. B.; Chen-Yong, L. *J. Biol. Chem.* **2000**, *275*, 36720.
4. Milner, J. M.; Patel, A.; Davidson, R. K.; Swingler, T. E.; Désilets, A.; Young, D. A.; Kelso, E. B.; Donell, S. T.; Cawston, T. E.; Clark, I. M.; Ferrell, W. R.; Plevin, R.; Lockhart, J. C.; Leduc, R.; Rowan, A. D. *Arthritis Rheum.* **2010**, *62*, 1955.
5. Cheng-Jueng, C.; Bai-Yao, W.; Pai-In, T.; Chi-Yung, C.; Mei-Hsuan, W.; Chan, Y. L. E.; Herng-Sheng, L.; Johnson, M. D.; Eckert, R. L.; Ya-Wen, C.; Chou, F.; Jehng-Kang, W.; Chen-Yong, L. *Am. J. Physiol. Cell Physiol.* **2011**, *300*, 406.
6. Netzel-Arnett, S.; Buzza, M. S.; Shea-Donohue, T.; Désilets, A.; Leduc, R.; Fasano, A.; Bugge, T. H.; Antalis, T. M. *Inflamm. Bowel Dis.* **2012**, *18*, 1303.
7. Beaulieu, A.; Gravel, É.; Cloutier, A.; Marois, I.; Colombo, É.; Désilets, A.; Verreault, C.; Leduc, R.; Marsault, É.; Richter, M. V. *J. Virol.* **2013**, *87*, 4237.
8. Baron, J.; Tarnow, C.; Mayoli-Nüssle, D.; Schilling, E.; Meyer, D.; Hammami, M.; Schwalm, F.; Steinmetzer, T.; Guan, Y.; Garten, W.; Hans-Dieter, K.; Böttcher-Friebertshäuser, E. *J. Virol.* **2013**, *87*, 1811.
9. Steinmetzer, T.; Schweinitz, A.; Stürzebecher, A.; Dönnecke, D.; Uhland, K.; Schuster, O.; Steinmetzer, P.; Müller, F.; Friedrich, R.; Than, M. E.; Bode, W.; Stürzebecher, J. *J. Med. Chem.* **2006**, *49*, 4116.
10. Steinmetzer, T.; Dönnecke, D.; Korsonewski, M.; Neuwirth, C.; Steinmetzer, P.; Schulze, A.; Saupe, S. M.; Schweinitz, A. *Bioorg. Med. Chem. Lett.* **2009**, *19*, 67.
11. Schweinitz, A.; Dönnecke, D.; Ludwig, A.; Steinmetzer, P.; Schulze, A.; Kotthaus, J.; Wein, S.; Clement, B.; Steinmetzer, T. *Bioorg. Med. Chem. Lett.* **2009**, *19*, 1960.
12. Colombo, É.; Désilets, A.; Duchêne, D.; Chagnon, F.; Najmanovich, R.; Leduc, R.; Marsault, E. *ACS Med. Chem. Lett.* **2012**, *3*, 530.
13. Galkin, A. V.; Mullen, L.; Fox, W. D.; Brown, J.; Duncan, D.; Moreno, O.; Madison, E. L.; Agus, D. B. *Prostate* **2004**, *61*, 228.
14. Goswami, R.; Mukherjee, S.; Wohlfahrt, G.; Ghadiyaram, C.; Nagaraj, J.; Beeram, R. C.; Sistla, R. K.; Satyam, L. K.; Dodheri, S. S.; Moilanen, A.; Hosahalli, S. S.; Ramachandra, M. *ACS Med. Chem. Lett.* **2013**, *4*, 1152.
15. Goswami, R.; Mukherjee, S.; Ghadiyaram, C.; Wohlfahrt, G.; Sistla, R. K.; Nagaraj, J.; Satyam, L. K.; Subbarao, K.; Palakurthy, R. K.; Gopinath, S.; Krishnamurthy, N. R.; Ikonen, T.; Moilanen, A.; Subramanya, H. S.; Kallio, P.; Ramachandra, M. *Bioorg. Med. Chem.* **2014**, *22*, 3187.
16. Friedrich, R.; Fuentes-Prior, P.; Ong, E.; Coombs, G.; Hunter, M.; Oehler, R.; Pierson, D.; Gonzalez, R.; Huber, R.; Bode, W.; Madison, E. L. *J. Biol. Chem.* **2002**, *277*, 2160.
17. *Procedure to determine inhibition constant (K_i)*: Cheng-Prusoff equation $K_i = IC_{50}/(1 + [S]/K_m)$ was used with experimentally determined IC_{50} and K_m values; where $[S]$ represents the substrate concentration and K_m Michaelis Menten constant.
18. Saleem, M.; Adhami, V. M.; Zhong, W.; Longley, B. J.; Chen-Yong, L.; Dickson, R. B.; Reagan-Shaw, S.; Jarrard, D. F.; Mukhtar, H. *Cancer Epidemiol. Biomarkers Prev.* **2006**, *15*, 217.